BMC Ecology and Evolution

Research article

Title: Rapid genomic evolution in *Brassica rapa* with bumblebee selection in experimental evolution

Authors: Léa Frachon[1, *], Florian P. Schiestl[1]

[1]Department of Systematic and Evolutionary Botany, University of Zürich, Zürich, Switzerland.

[*]***Corresponding author***:

Léa Frachon

lea.frachon@systbot.uzh.ch

Abstract

Background. Insect pollinators shape rapid phenotypic evolution of traits related to floral attractiveness and plant reproductive success. However, the underlying genomic changes remain largely unknown despite their importance in predicting adaptive responses to natural or to artificial selection. Based on a nine-generation experimental evolution study with fast cycling *Brassica rapa* plants adapting to bumblebees, we investigate the genomic evolution associated with the previously observed parallel phenotypic evolution. In this current evolve and resequencing (E&R) study, we conduct a genomic scan of the allele frequency changes along the genome in bumblebee-pollinated and hand-pollinated plants and perform a genomic principal component analysis (PCA).

Results. We highlight rapid genomic evolution associated with the observed phenotypic evolution mediated by bumblebees. Controlling for genetic drift, we observe significant changes in allelic frequencies at multiple loci. However, this pattern differs according to the replicate of bumblebee-pollinated plants, suggesting putative non-parallel genomic evolution. Finally, our study underlines an increase in genomic differentiation implying the putative involvement of multiple loci in short-term pollinator adaptation.

Conclusions. Overall, our study enhances our understanding of the complex interactions between pollinator and plants, providing a steppingstone towards unravelling the genetic basis of plant genomic adaptation to biotic factors in the environment.

Key words: fast cycling *Brassica rapa*, experimental evolution, evolve and resequencing study, non-parallel genomic evolution, rapid genomic evolution, bumblebees' selection.

Background

Pollinator insects are important selective agents for wild- and crop plant species due to their essential role in the reproduction of most flowering plants [1]. While a decline of pollinator insects has been detected in different geographical regions and insect families [2, 3, 4], the understanding of the adaptive potential of plants to such changes remains in its infancy. Plant adaptation to pollinators typically involves traits associated with flower attractiveness such as (1) flower morphology [5, 6, 7], flower colour [8, 9], flower scent [10, 11, 12], and (2) traits associated with mating system like herkogamy [13, 14] or selfing [15, 16]. While most studies assessed the result of long-term evolutionary adaptation to pollinators, tracking the adaptive processes across generations remains scarce. Both the resurrection approach in natural populations, growing seeds from different generations together, or experimental evolution studies, applying the same selective pressure for multiple generations, can bridge this gap. For instance, using a resurrection approach, Thomann et al. (17) observed phenological and reproductive trait changes over 18 years in *Adonis annua* plants in response to the loss of wild bees. While this approach benefits from ecological realism in natural populations, it makes it difficult to differentiate the effect of the factor of interest from other factors such as climate, also shaping plant evolution. Gervasi and Schiestl [12] performed experimental evolution with fast-cycling *Brassica rapa* plants evolving with different pollinators and under controlled conditions, to identify the evolutionary response to pollinator-mediated selection. They showed, within nine generations of experimental evolution, rapid plant adaptation to bumblebee pollination in phenotypic traits, such as floral volatiles, UV reflection and plant height. However, while these evolved traits have also been shown to carry substantial heritability in this study system [18, 19], the genomic changes underlying these rapid plant phenotypic changes are still unknown.

In the current context of pollinator decline and the associated changes in pollinator communities, understanding the genetic architecture involved in plant response to pollinators is

57 essential to understand their adaptative potential in changing environments [20, 21, 22]. Molecular
58 genetic studies have uncovered the molecular and genetic bases of several traits involved in pollination
59 and pollinator attractiveness such as selfing [23], pollination syndromes [24, 8, 25, 26, 27], nectar [28,
60 29] and volatiles [30, 31, 32, 33, 34]. However, insects use a combination of signals (shape, colour,
61 scent) and rewards for identifying suitable flowers leading to plant adaptation based on multiple traits
62 [35]. For instance, honest signals (signals associated with reward) and pollination syndromes
63 (convergent evolution of specific signal combinations selected by pollinators) are good examples of
64 evolution of multiple traits. In a context of rapid environmental changes, genetic correlation among
65 traits may allow the synchronous response of different phenotypic traits to varying patterns of
66 selection [36, 37, 19]. While essential to predict the adaptive potential of plants to pollinators and
67 enable breeding of crop that are more attractive to pollinators, we are still in the beginning of
68 understanding the genetic basis involved in the adaptative response to pollinators . By combining
69 experiment evolution and next generation sequencing (NGS), evolve and resequencing (E&R) studies
70 have proven their ability to unravel the genomic basis involved in rapid evolution [38, 39, 40].

71 Here, based on previous experimental evolution performed by Gervasi and Schiestl [12] with
72 outcrossing fast-cycling *Brassica rapa* plants, we tracked the genomic changes involved in the
73 adaptative response of plants to bumblebee selection compared to hand pollinated control plants in
74 an E&R study (**Figure 1**). Gervasi and Schiestl [12] initiated their experimental evolution with 108 full
75 sib seed families in the greenhouse. Over nine generations of selection, they grew plants in three
76 isolated replicates (36 plants per replicate). The selection was mediated by three pollination
77 treatments during the experiment: bumblebee (*Bombus terrestris*) pollination, hoverfly- (*Episyrphus*
78 *balteatus*), and hand pollination. Overall, they observed parallel phenotypic evolution with
79 bumblebee-pollinated plants evolving taller, more fragrant flowers, and being more attractive to
80 bumblebees. In our E&R study, we re-sequenced plants from two replicates in bumblebee and hand-

81 pollination treatments. We performed a genome scan of allele frequency changes and a genomic

82 principal component analysis to observe putative genomic evolution shaped by bumblebees.

83

84 **Figure 1**

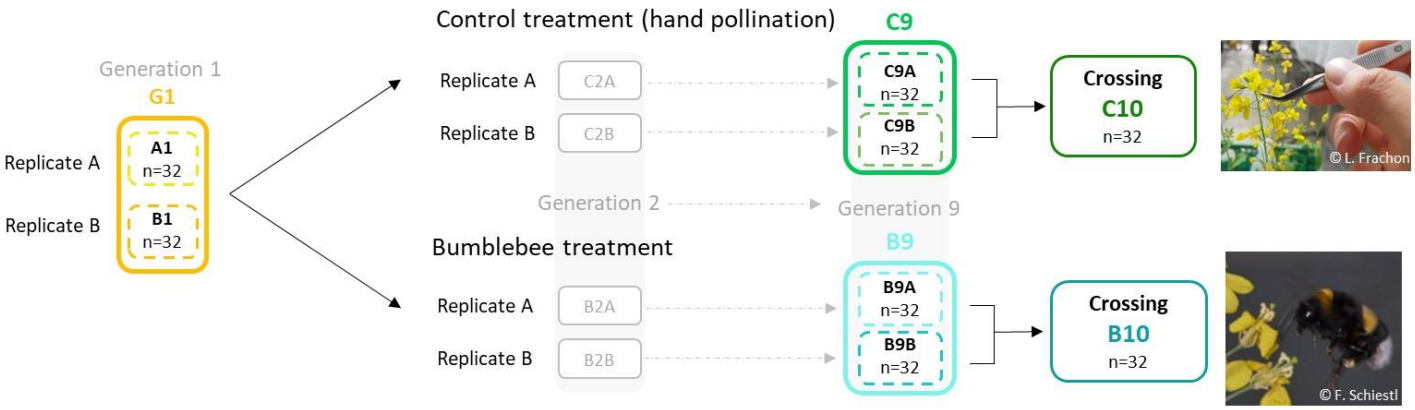

85

86 **Results**

87 **Genomic changes during experimental evolution.** In our study, we observed allele frequency changes

88 (Δh) over nine generations in both bumblebee and control treatments and between two replicates

89 within treatments (**Figure 2**). Based on 10'000 genetic drift simulations, we defined significant changes

90 (colored dots in **Figure 2**) as observed changes in allele frequency outside the drift simulation ranges

91 (upper and lower grey lines in **Figure 2**). The allele frequency changes varied substantially between

92 treatments and between replicates within treatments. For instance, we found 32 SNPs with strong

93 ($\Delta h > 0.5$) and significant (fdr < 0.05) changes in one of the replicates of the bumblebee treatment

94 (replicate A). In contrast, we observed only 4 SNPs with significant allele frequency changes in the

95 other replicate in bumblebee treatment (replicate B). In the control (hand-pollinated) treatment,

96 there were 3 SNPs with significant allele frequency changes in one replicate (B) and zero SNPs with

97 allele frequency changes in the other replicate (A). In replicate A, we found a 42-fold increase in the

98 number of SNPs displaying significant allele frequency changes (fdr > 0.05) with the bumblebee
99 treatment compared to the control treatment, regardless of its strength i.e. considering all the value
100 of Δ*h* (4 SNPs with significant changes in the control treatment, and 171 SNPs in the bumblebee
101 treatment, **Figure 2**). However, no difference in the number of SNPs involved in significant allele
102 frequency changes between bumblebee and control treatment were observed in replicate B (21 SNPs
103 with significant changes in the control, and 19 SNPs in the bumblebee treatment considering fdr < 0.05,
104 considering all value of Δ*h*, **Figure 2**).

105 **Figure 2**

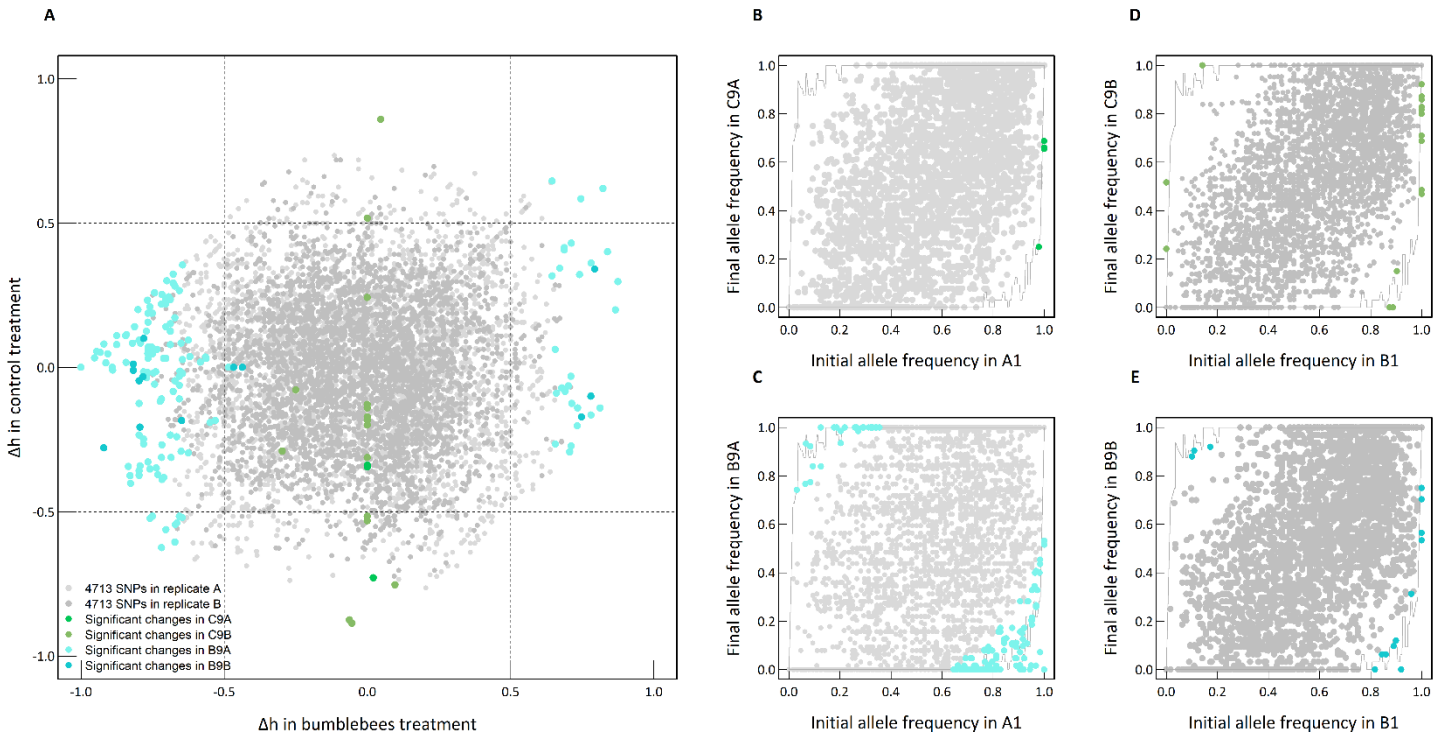

106

107 As expected, the evolutionary process is associated with an increase of linkage disequilibrium
108 in the bumblebee treatment, but also in the control treatment. In both treatments, we observed a
109 slower decay of the median linkage disequilibrium in the ninth generation compared to the first
110 generation (**Figure S3A**). Within the bumblebee treatment, we observed a slower decay of LD in

111 replicate A than in B as expected with the observed stronger allele frequency changes (**Figure S3A**).
112 The decays of LD in inter-replicate crossing were slower in both treatments compared to the ninth
113 generation (**Figure S3A**). Moreover, we observed a decrease of the number of haplotype blocks, *i.e.*,
114 genomic regions with strongly linked alleles, over nine generations (from 786 and 780 haplotype blocks
115 for replicate A and B respectively in the first generation, to 563 and 648 haplotype blocks for replicate
116 A and B respectively in the ninth generation of the control treatment, and 478 and 600 for replicate A
117 and B respectively in the ninth generation of the bumblebee treatment) associated with an increase
118 of their length (**Figure S3BC**, **Table S1**). We observed 743 and 696 haplotype blocks in control and
119 bumblebee treatments respectively in the inter-replicate crossing (**Figure S3BC, Table S1**). It is worth
120 noting that the moderate density of genetic markers (18 SNPs per Mb in mean among the 10
121 chromosomes, **Figure S1**) suggests that the estimate of LD and haplotype length may be slightly
122 underestimated, although this has no effect on the trends observed.

123 Overall, the SNPs involved in the evolutive responses are independent between replicates, and
124 between treatments (**Figure 3**). For instance, among the 171 SNPs with significant allele frequency
125 changes in replicate A in bumblebee treatment, 164 SNPs are unique of this population, whereas 5
126 SNPs are shared with the control treatment in replicate B, and 3 SNPs are shared with the bumblebee
127 treatment in replicate B (**Figure 3**).

128

129

130

131

132

133

134 **Figure 3**

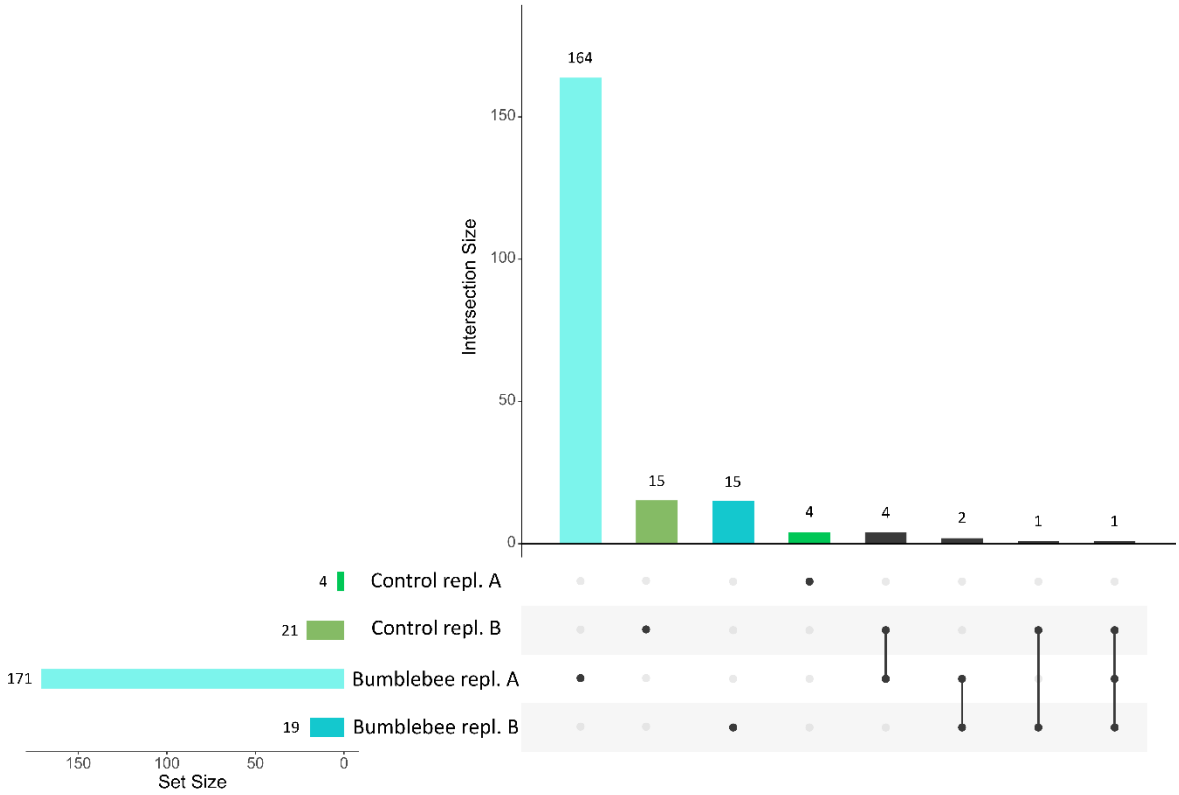

135

136

137 **Identity of candidate genes underlying genomic evolution in bumblebee treatment.** After retrieving
138 the annotated genes around 4kb (2kb upstream, 2kb downstream) for 187 SNPs with significant allele
139 frequency changes in the bumblebee treatment (fdr < 0.05), we obtained a list of 171 candidate genes
140 (**Dataset1**). Briefly, we found genes with biological functions that may be involved in the emission of
141 volatiles (ABC transporter G), in the regulation of flowering time (B3), or in shoot architecture (UCH).
142 In addition, some genes are involved in the response to different biotic and abiotic stresses
143 (METACASPASE-2, PUB, Pum, PAT8, BON). Finally, some candidate genes do not have a known
144 biological function. However, due to a putative underestimate of LD and haplotype length (see
145 previous section), we may not have been able to correctly identify all the candidate genes involved in
146 this evolutionary process. **Genome-wide population structure.** To assess the relatedness among

147 individuals across generation and treatments, we performed a genomic principal component analysis
148 (PCA) on the full set of SNPs (4'713 SNPs). We observed a structuration of our samples determined by
149 populations *i.e*. generations, treatments, and replicates (**Figure 4**). Along the six first principal
150 components (PCs) axis, explaining 56.07% of the total genomic variance (**Figure 4A**), all individuals
151 from the two replicates of generation one were grouped together, and individuals from the ninth
152 generations were clearly separated from the first generation (**Figure 4**). In this genomic space,
153 individuals from the inter-replicate crossing fell between those from the scatterplot formed by
154 replicates A and B of generation nine for both treatments (**Figure 4**). Interestingly, in the genomic space
155 created by the first 6 principal components explaining the most genetic variance, the individuals
156 resulting from selection by bumblebees were always more scattered than those from the control
157 treatment or the first generation.

158

159

160

161

162

163

164

165

166

167

168

169 **Figure 4**

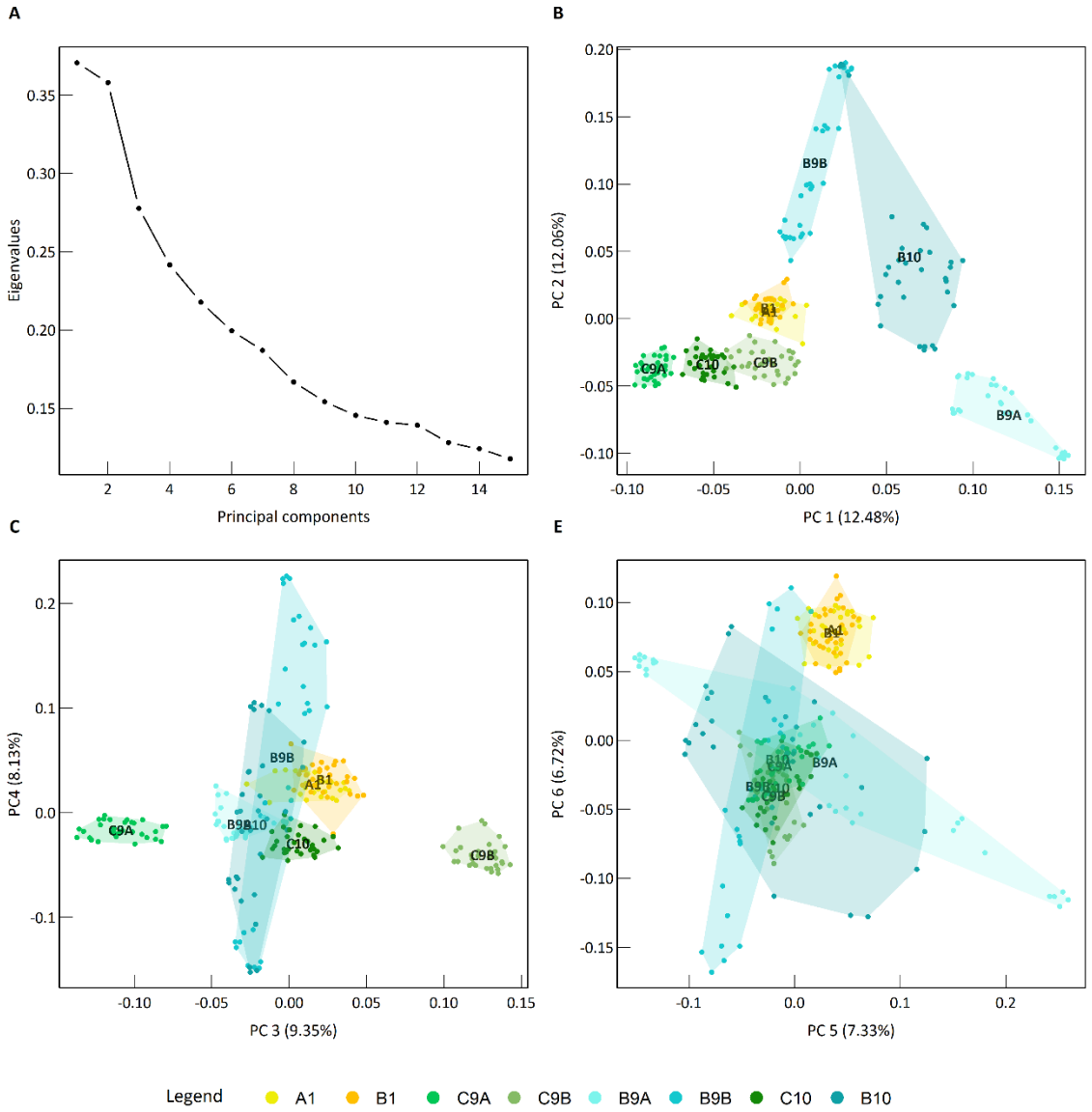

170

171

172 **Discussion**

173 Understanding pollinator-mediated evolutionary genomics of flowering plants remains an
174 important challenge in biodiversity conservation and crop improvement. Here, we screened for the
175 genomic consequences of biotic selection in an E&R study by sequencing genome-wide SNP markers

176 in *Brassica rapa* plant individuals before and after nine generations of selection by bumblebees, and
177 under random hand-pollination. The previous experimental evolution has shown, at the phenotypic
178 level, that this primarily outcrossing plant rapidly adapts to specific pollinators [12]. For instance,
179 Gervasi and Schiestl [12] observed taller plants with an increase in total scent emission per flower in
180 bumblebee-pollinated plants. The pattern of phenotypic evolution was similar between replicates
181 from the same pollination treatment. In this E&R study, we documented the putative signature of
182 directional selection driven by bumblebee pollinators with significant allele frequency changes at
183 several loci. Moreover, we have shown different pattern of genomic evolution between replicates, and
184 an increase of genomic differentiation among individuals.

185 In agreement with the demonstrated phenotypic evolution in the fast-cycling *Brassica rapa*
186 experimental system [12], we have shown genomic evolution across nine generations. The here
187 documented changes in allele frequencies, the increase of linkage disequilibrium and the number of
188 haplotype blocks, underscore the importance of pollinators in shaping plant rapid genomic evolution.
189 The limited number of individuals (36 per replicate and per treatment) and replicates (2 replicates)
190 could impact the evolutionary processes and the identification of the underlying genomic bases.
191 Indeed, small population size can lead to an increase in the effect of genetic drift, and a low number
192 of replicates to a poor estimate of loci under selection [41]. However, at the phenotypic level, the
193 observed differences among the three replicates were smaller than those observed among treatments,
194 indicating that pollinator selection played a larger role than random drift [12]. Moreover, in our study,
195 we accounted for genetic drift bias and identified changes in allele frequency that were greater than
196 those expected from 10'000 genetic drift simulations. While we cannot completely exclude some
197 effects of genetic drift, this alone cannot explain the patterns observed. Moreover, some significant
198 candidate genes identified in our E&R study have biological functions in line with the phenotypic
199 evolution of traits observed by Gervasi and Schiestl [12]. For instance, while the previous experimental
200 evolution study highlighted an increase in scent emission and plant height driven by bumblebee

201 pollination, we identified candidate genes who, or at least their family, are known to be involved in
202 emission of volatile organic compounds, like ABC transporter G family (ABCG35, ABCG38, ABCG1,
203 ABCB19, [42, 43]), in shoot architecture like Ubiquitin C-terminal hydrolase (UCH [44]), or in growth
204 and development like AUXIN-RESPONSIVE PROTEIN-RELATED, or TREHALOSE-PHOSPHATE
205 PHOSPHATASE E-RELATED [45]. The U-box protein is also an interesting candidate gene due to its
206 involvement in different developmental and physiological processes such as self-incompatibility,
207 defence, or abiotic stress response [46]. Moreover, we found significant allele frequency changes
208 associated with flowering time like a B3 transcription regulator [47] or UCH [48]. While Gervasi &
209 Schiestl [12] did not observe any difference in flowering time between bumblebee and control
210 treatment in the last generation, flowering time is an important phenological trait involved in plant-
211 pollinator matching [49, 50]. It is therefore possible that pollinators induce flower phenological shift,
212 which was not detected in the phenotypic data, but picked up in the genomic changes as changes
213 influencing flowering time. Overall, our study highlighted the potential involvement of multiple loci in
214 rapid adaptation to bumblebees, which agrees with studies highlighting such a genetic architecture
215 underlying floral evolution [51, 26,52, 37,53]. However, further analysis using higher quality of
216 sequencing and the characterization of associated phenotypic and phenological traits (allowing a
217 genome-wide association approach) and functional validation of the genes are required to draw more
218 solid conclusions about the genetic basis of evolutionary changes induced by bumblebee selection.

219 In addition, we found that the extent of genomic changes observed during the evolutionary
220 processes was different between replicates suggesting non-parallel genomic evolution [54]. While
221 Gervasi and Schiestl [12] have shown convergent (or parallel) phenotypic evolution for the bumblebee
222 treatment, our results indicated that only one replicate exhibited several loci with significant changes
223 in allele frequency (i.e. outside the range of drift simulations). Such a convergent phenotypic evolution
224 associated with non-parallel genomic evolution has been observed in artificial selection of crops [55,
225 56] and in natural populations. For instance, a recent study highlighted different genomic regions

226 underpinning the evolutionary convergence of herbicide resistance in blackgrass among different
227 populations [57]. Likewise, in natural populations of *Senecio lautus,* similar phenotypic variation was
228 reported to be regulated by variation in genomic space across populations in dune-headland coastal
229 habitats [58]. However, the low number of replicates in our study and the significant changes in allele
230 frequencies observed in only one replicate do not provide a clear distinction between potential non-
231 parallel evolution and a "two-speed" parallel genomic evolution (*i.e.* the second replicate will follow
232 the same evolutionary path in the upcoming generations). Longer experimental evolution, with more
233 replicates and individuals are needed to clearly understand the evolutionary pattern mediated by
234 biotic factors such as bumblebees.

235 Finally, we observed an increase of genomic variance, within the genomic space created by the
236 main differentiation axes, during experimental evolution mediated by bumblebees [12]. This increase
237 in overall genomic variance was observed among individuals in both bumblebee-pollinated replicates
238 (B9A and B9B), as well as in the inter-replicate crossing (B10). This pattern might be explained by the
239 polygenic model with a weaker selection acting on multiple standing variants (soft sweep) and by
240 multiple loci underlying individual phenotypic trait evolutionary changes. An increased number of
241 studies demonstrate the importance of polygenic adaptation [56, 60, 61, 62] related to the
242 infinitesimal model (reviewed in Barton et al. [63]), where local adaptation is driven by small allele
243 frequency changes in multiple loci. Interestingly, highly polygenic architecture involved in phenotypic
244 evolution could contribute to the maintenance of standing genetic variation, as recently demonstrated
245 in long-term artificial selection on chicken weight [64]. However, deepened analyses are needed using
246 newly developed models to validate the involvement of polygenic architecture in rapid phenotypic
247 evolution [65, 66, 67]. Multiple genes underlying phenotypic variation are widely emphasized in plants
248 with the advances of GWAs [59, 62], however the interplay of evolutionary forces on these genes is
249 still poorly understood and deserves further studies.

Conclusion

We revealed important genomic changes on multiple loci associated with convergent phenotypic evolution resulting from bumblebee selection in only nine generations. Our study is a first step into the understanding of the complex genomic mechanisms involved in rapid evolutionary adaptation to biotic factors, and we advocate further analyses to understand (1) the genetic architecture underlying phenotypic and phenological variation, (2) pleiotropic effects of quantitative-trait locus in rapid adaptation and (3) the mechanisms behind a maintenance of genetic variance. We also underline the importance of better characterizing the gene functions involved in plant-pollinator interactions. Overall, pollinators constitute complex patterns of selection which deserve more attention for predicting the adaptive responses of wild and crop plant species to their decline.

Methods

Plant material and experimental design. *Brassica rapa* (Brassicacea) is an outcrossing plant with genetic self-incompatibility, pollinated by diverse insects such as bumblebees, flies or butterflies [68]. Our study used rapid-cycling *Brassica rapa* plants (Wisconsin Fast Plants™, purchased from Carolina Biological Supply Company, Burlington, USA), selected for its short life cycle of approximately two months from seed to seed in our greenhouse conditions. We used seeds produced by the study of Gervasi and Schiestl [12], performing experimental evolution with bumblebees and control hand pollination. Briefly, starting from 108 full sib seed families, the pollination was carried out over nine generations either by bumblebees (*Bombus terrestris*), hoverflies (*Episyrphus balteatus*) or by random hand cross-pollination (control treatment). This experiment was conducted with 3 isolated replicates (one replicate includes 36 plants) for each treatment. A representative subset of seeds from all pollinated flowers was used for the next generation; the contribution of seeds to the next generation being calculated as 36 divided by the sum of seeds per replicate over all individual seeds. In this study,

274 we focused on bumblebee and hand-pollination treatment, using two most distinct replicates
275 (replicate A and B). We used the offspring of the starting populations and the ninth generation for both
276 treatments. On seed per individual plant were used. In total, we used 32 32 plants from the starting
277 generation (generation 1) in replicate A (called A1), and 32 plants from replicate B (called B1), 32 plants
278 from the ninth generation selected by bumblebees (bumblebee treatment) in replicate A (called B9A)
279 and 32 plants in replicate B (called B9B)and ; 32 plants from the ninth generation of control hand
280 pollination plants (control treatment) in replicate A (called C9A) and replicate B (C9B; **Figure 1**). Finally,
281 we performed crossings between replicates A and B within each treatment (generation 10) yielding 32
282 individuals from the bumblebee treatment (inter-replicate crossing in bumblebee treatment; here
283 called B10) and 32 individuals from the control treatment (inter-replicate crossing in control
284 treatment; here called C10). This manual crossing is commonly used for reducing the effect of potential
285 inbreed depression on trait changes. Pollen donors and receivers were randomly assigned. Each
286 combination of generation*treatment*replicate is called a population (*e.g.* ninth generation,
287 treatment bumblebees, replicate A called B9A is a population). A total of 256 seeds from these 8
288 populations (first, ninth and tenth generation) were sown out in a phytotron (first generation in 2017
289 and ninth generation as well as the inter-replicate crossing in 2019) and the leaf tissue of each plant
290 was collected for DNA extraction and whole genomic sequencing. The study conforms to the
291 institutional, national, and international regulations.

292

293 **DNA extraction and genomic characterization.** Because leaf tissue was collected in 2017 for the first
294 generation and 2019 for the last generations, we adapted the collection storage (drying vs freezing).
295 Leaf material from the first generation was dried in vacuum at 40 °C for 20 hours, and leaf material
296 from the ninth and tenth generation was stored in -80°C. A high molecular weight DNA extraction
297 (average DNA concentration of 48 ng/µL, LGC extraction protocol) and library preparation for

298 genotyping-by-sequencing (restriction enzyme MsII, insert size mean range ~215bp) was performed
299 by the LGC Genomics group Berlin. Samples were sequenced with Illumina NextSeq 500 V2 sequencer
300 using 150 paired-end reads; the alignment of our samples was performed with BWA version 0.7.12
301 against the reference genome sequence of *Brassica rapa* FPsc v1.3, Phytozome release 12
302 (https://phytozome.jgi.doe.gov/pz/portal.html) by the LGC Genomics group Berlin. The variant
303 discovery and the genotyping were realized using Freebayes v1.0.2-16 with the following parameters
304 by the LGC Genomic Group Berlin: --min-base-quality 10 –min-supporting-allele-qsum 10 –read-
305 mismatch-limit 3 –min-coverage 5 –no-indels –min-alternate-count 4 –exclude-unobserved-genotypes
306 –genotype-qualities –ploidy 2 or 3 –no-mnps –no-complex –mismatch-base-quality-threshold 10. We
307 then performed a quality trimming on the 10 chromosomes *i.e.* by discarded unassigned scaffolds from
308 the chromosomes using vcftools [69], by removing SNPs with missing data in more than 5% of the
309 individuals (function –max-missing 0.95, *i.e.* genotype calls had to be present for at least 243 samples
310 out of 256 for a SNP to be included in the downstream analysis), and retaining only bi-allelic SNPs with
311 a minimum average Phred quality score of 15 (function –minGQ 15, **Figure S2DE**). We removed SNPs
312 with a maximum average read depth of 100 (function –max-meanDP 100, **Figure S2BC**), and discarded
313 SNPs with a minor allele frequency (MAF) lower than 0.1 (function –maf 0.1, **Figure S2A**). The final
314 dataset contained 4'713 SNPs in ~ 283Mb genome size
315 (https://phytozome.jgi.doe.gov/pz/portal.html).

316 **Allele frequency changes and genetic drift simulation**. The allele frequencies of the reference allele
317 for the 4'713 SNPs were estimated within each 8 populations using vcftools (function –freq, [64]). To
318 control potential genetic drift during the nine generations of evolution, we simulated random final
319 allele frequencies 10'000-fold for different ranges of initial allele frequencies (from 0 to 1 by an interval
320 window of 0.01). The simulations were performed using the R environment package "learnPopGen"
321 (function "drift.selection", [70]) over eight transitions between generations (*i.e.* from the first
322 generation to the ninth generation) considering 32 individuals within each population for an effective

size (N_e) of 16 (*i.e.* individuals contributing to the next generation, see details of experimental evolution in Gervasi and Schiestl [12]), and considering an equal fitness for each individual. For each SNP along the genome, we assigned their initial allele frequency value ($AF_{initial}$) to the range estimated by the final allele frequency simulations (10'000 values). Finally, the observed final allele frequency (AF_{final}) was compared to 10'000 simulated allele frequency values ($AF_{simulated}$) to estimate a p-value for each SNP using the following equations:

(1) For a decrease of reference allelic frequency *i.e.* ($AF_{initial} - AF_{final}$) > 0, *pvalue* = (number of simulations with $AF_{simulated} \geq AF_{final}$)/10'000

(2) For an increase of reference allelic frequency *i.e.* ($AF_{initial} - AF_{final}$) < 0, *pvalue* = (number of simulations with $AF_{simulated} \leq AF_{final}$)/10'000

(3) For ($AF_{initial} - AF_{final}$) = 0, *pvalue* = 1

With $AF_{simulated}$ = simulated final allele frequency, $AF_{initial}$ = initial allele frequency from the reference allele (first generation), and AF_{final} = observed final allele frequency for the reference allele (ninth generation). The pvalues were controlled for the False Discovery Rate (fdr) of 5% using Benjamini-Hochberg method implemented in R environment [71].

Finally, we estimated the allele frequency changes (Δh) from the reference allele according to the equation (1) for both bumblebee and control treatments:

$$\Delta h = \mathrm{AF}_{\mathrm{final}} - \mathrm{AF}_{\mathrm{initial}} \qquad (1)$$

Where Δh is the allelic frequency change between the first and the ninth generation, $AF_{initial}$ is the initial observed allele frequency, and AF_{final} is the observed final allele frequency at the ninth generation.

Linkage disequilibrium (LD) and haplotype block structure evolution. During the selective process, an increase of the linkage disequilibrium *i.e.* the non-random association of alleles between loci, is expected in genomic regions strongly under selection. First, we calculated pairwise linkage

346 disequilibrium (LD) among all set of SNPs measured by the correlation coefficient between SNP pair r^2
347 within each chromosomes using VCFtools (function –geno-r2) for each 8 populations containing 32
348 individuals. The associated median LD was then estimated and plotted. Finally, to understand whether
349 changes in median LD are due to random allelic associations along the genome, or aggregated in
350 genomic regions under selection, we calculated the haplotype blocks in each population using plink1.9
351 with the following parameters: --blocks no-pheno-req –maf 0.07 –blocks-max-kb 200. This method
352 estimates the length of these blocks with "strong LD" considering the allelic association D' metrics
353 between 0.7 and 0.98 according to Gabriel et al. [72].

354 **Candidate genes.** We identified 171 candidate genes associated with 187 SNPs with significant allele
355 frequency changes (fdr < 0.05) during bumblebee selection. Because the median linkage disequilibrium
356 in bumblebee treatment is ~4kb, we retrieved the annotated genes around 4kb (2 kb upstream and 2
357 kb downstream) for 187 SNPs and extracted the gene description using phytozome.jgi.doe.gov.

358 **Genome-wide variance changes.** The genomic variance among individuals within each population was
359 estimated using principal component analysis (PCA) on scaled and centered genotype data (pcadapt
360 package in R environment, function pcadapt, [73]). In order to unravel the changes in genomic variance
361 over nine generations, we performed the PCA (1) on the total number of SNPs (4713 SNPs), and (2) on
362 187 SNPs showing significant allele frequency changes under bumblebee selection in on or another
363 replicate (fdr < 0.05). To compare genomic variance among populations, we estimated the area of the
364 polygon formed by scatter plots of axis 1 and 2 of each population for the full dataset (4713 SNPs) and
365 the subset of 187 SNPs using R package tidyverse and splancs [74, 75]. The relative area is the ratio
366 between the polygon area within each population and the polygon area circumventing all the points
367 of the PCA.

368
369
370

Declarations

Ethics approval and consent to participate. The study conforms to the institutional, national, and international regulations.

Consent for publication. Not applicable.

Availability of data and material. The datasets used and/or analysed during the current study are available from the corresponding author on reasonable request. The DNA sequences of all samples will be available at National Library for Biotechnology Information (NCBI) database (BioProject PRJNA931117) after acceptance of the manuscript. Reviewers can access to the data using the following link:
https://dataview.ncbi.nlm.nih.gov/object/PRJNA931117?reviewer=hocdpu4je8n22ueldu7potnjqn

Competing interests. The authors declare that they have no competing interests.

Funding. University of Zürich provided funding.

Authors' contributions. L.F. and F.S. designed the research. L.F. performed the DNA extraction and statistical analyses and wrote the manuscript. L.F. and F.S. reviewed and edited the manuscript.

Acknowledgements

We thank Jörg Vogt for the first-generation DNA extraction, and the LGC Genomic group Berlin for the DNA extraction of other samples, the sequencing and bioinformatic treatment. We thank Cyril Zipfel for discussion regarding candidate genes. We thank Loren Rieseberg and Marius Rösti for their useful comments on a previous version of the draft. Finally, we thank the University of Zürich for their financial support.

References

1. Van der Niet T, Peakall R, Johnson SD. Pollinator-driven ecological speciation in plants: new evidence and future perspectives. *Ann Bot*. 2014;113:199–211.
2. Biesmeijer JC, et al. Parallel declines in pollinators and insect-pollinated plants in Britain and the Netherlands. *Science*. 2006;313:351-354.
3. Hallmann C, et al. More than 75 percent decline over 27 years in total flying insect biomass in protected areas. *PloS ONE*. 2017;12:e0185809.
4. Wagner DL, Grames EM, Forister ML, Berenbaum MR, Stopak D. Insect decline in the Anthropocene: Death by a thousand cuts. *Proc. Natl. Acad. Sci. U.S.A*. 2020;118:e2023989118.
5. Anderson B, Pauw A, Cole WW. Barrett SCH. Pollination, mating and reproductive fitness in a plant population. *J. Evol. Biol*. 2016;29:1631–1642.
6. Wessinger CA, Hileman LC. Accessibility, constraint, and repetition in adaptive floral evolution. *Dev. Biol*. 2016;419:175–183.
7. Minnaar C, Anderson V, de Jager ML, Karron JD. Plant–pollinator interactions along the pathway to paternity. *Ann. Bot*. 2019;123:225–245.
8. Bradshaw HD, Schemske DW. Allele substitution at a flower colour locus produces a pollinator shift in monkeyflowers. *Nature*. 2003;426:176-178.
9. Sobral M, Veiga T, Domínguez P, Guitián JA, Guitián P, Guitián JM. Selective pressures explain differences in flower color among Gentiana lutea populations. *PloS ONE*. 2015;10:e0132522.
10. Schiestl FP. On the success of a swindle: pollination by deception in orchids. Sci. Nat. 2005;92:255–264.
11. Xu S, Schlüter PM, Grossniklaus U, Schiestl FP. The genetic basis of pollinator adaptation in a sexually deceptive Orchid. *PloS Genet*. 2012;8:e1002889.
12. Gervasi DDL, Schiestl FP. Real-time divergent evolution in plants driven by pollinators. *Nat. comm*. 2017;8:14691.
13. Moeller DA, Geber MA. Ecological context of the evolution of self-pollination in *Clarkia xantiana*: population size, plant communities, and reproductive assurance. *Evolution*. 2005;59:786–799.
14. Luo Y, Widmer A. Herkogamy and its effects on mating patterns in *Arabidopsis thaliana. PloS ONE*. 2013;8: e57902.
15. Bodbyl Roles SA, Kelly JK. Rapid evolution caused by pollinator loss in *Mimulus guttatus. Evolution*. 2011;65:2541–2552.
16. Ramos SE, Schiestl FP. Rapid plant evolution driven by the interaction of pollination and herbivory. *Science*. 2019;364:193–196.
17. Thomann M, Imbert E, Cheptou PO. Is rapid evolution of reproductive traits in Adonis annua consistent with pollinator decline? *Acta Oecol*. 2015;69:161-166.
18. Zu P, Blanckenhorn WU, Schiestl FP. Heritability of floral volatiles and pleiotropic responses to artificial selection in *Brassica rapa*. *New Phytol*. 2016;209:1208–1219.
19. Zu P, Schiestl FP. The effects of becoming taller: direct and pleiotropic effects of artificial selection on plant height in Brassica rapa. *Plant J*. 2017;89:1009–1019.
20. Hansen TF. The evolution of genetic architecture. *Annu. Rev. Ecol. Evol. Syst*. 2006;37:123–57.
21. Bergelson J, Roux F. Towards identifying genes underlying ecologically relevant traits in Arabidopsis thaliana. *Nat. Rev. Genet.* 2010;11:867-879.
22. Bay RA, et al. Predicting responses to contemporary environmental change using evolutionary response architectures. *Am. nat*. 2017;189:463-473.
23. Sicard A, Lenhard M. The selfing syndrome: a model for studying the genetic and evolutionary basis of morphological adaptation in plants. *Ann. Bot*. 2011;107:433–1443.
24. Bradshaw HD, Wilbert SM, Otto KG, Schemsket DW. Genetic mapping of floral traits associated with reproductive isolation in monkeyflowers (*Mimulus*). *Nature*. 1995;376:762-765.

452 25. Streisfeld MA, Rausher MD. Genetic changes contributing to the parallel evolution of red floral
453 pigmentation among Ipomoea species. *New Phytol*. 2009;183:751–763.
454 26. Yuan YW, Byers KJRP, Bradshaw HDJ. The genetic control of flower–pollinator specificity. *Curr.*
455 *Opin. Plant Biol*. 2013;16:422–428.
456 27. Yarahmadov T, Robinson S, Hanemian M, Pulver V, Kuhlemeier C. Identification of transcription
457 factors controlling floral morphology in wild Petunia species with contrasting pollination
458 syndromes. *Plant J*. 2020;104:289–301.
459 28. Lin W, *et al*. Nectar secretion requires sucrose phosphate synthases and the sugar transporter
460 SWEET9. *Nature*. 2015;508:546-549.
461 29. Solhaug EM, et al. An integrated transcriptomics and metabolomics analysis of the Cucurbita pepo
462 nectary implicates key modules of primary metabolism involved in nectar synthesis and
463 secretion. *Plant Direct*. 2019;3:e00120.
464 30. Dudareva N, Negre F, Nagegowda DA, Orlova I. Plant Volatiles: Recent Advances and Future
465 Perspectives. *Crit. Rev. Plant Sci*. 2006;25:417–440.
466 31. Klahre U, *et al*. Pollinator choice in Petunia depends on two major genetic loci for floral scent
467 production. *Curr. Biol*. 2011;21:730-739.
468 32. Cai J, Zu P, Schiestl FP. The molecular bases of floral scent evolution under artificial selection:
469 insights from a transcriptome analysis in Brassica rapa. *Scientific Reports*. 2016;6:36966.
470 33. Fattorini R, Glover BJ. Molecular Mechanisms of Pollination Biology. *Ann. Rev. Plant Biol*.
471 2020;71:487-515.
472 34. Lo S, Fatokun C, Boukar O, Gepts P, Close TJ, Muñoz-Amatriain M. Identification of QTL for
473 perenniality and floral scent in cowpea (*Vigna unguiculata* [L.] Walp.). *PloS ONE*.
474 2020;15:e0229167.
475 35. Schiestl FP, Johnson SD. Pollinator-mediated evolution of floral signals. *Trends in Ecology &*
476 *Evolution*. 2013;28:307-315.
477 36. Hermann K, Klahre U, Moser M, Sheehan H, Mandel T, Kuhlemeier C. Tight genetic linkage of
478 prezygotic barrier loci creates a multifunctional speciation island in *Petunia*. *Curr. Biol*.
479 2013;23:873–877.
480 37. Smith SD. Pleiotropy and the evolution of floral integration. *New Phytologist*. 2015;209:80–85.
481 38. Turner TL, Stewart AD, Fields AT, Rice WR, Tarone AM. Population-based resequencing of
482 experimentally evolved populations reveals the genetic basis of body size variation in
483 *Drosophila melanogaster. PLoS Genet.* 2011; 7:e1001336.
484 39. Schlötterer C, Kofler R, Versace E, Tobler R, Franssen SU. Combining experimental evolution with
485 next-generation sequencing: a powerful tool to study adaptation from standing genetic
486 variation. *Hered*. 2015;114:431-440.
487 40. Long A, Liti G, Luptak A, Tenaillon O. Elucidating the molecular architecture of adaptation via
488 evolve and resequence experiments. *Nat. Rev. Genet*. 2015;16:567-582.
489 41. Kofler R, Schötterer C. A guide for the design of evolve and resequencing studies. *Mol. Biol. Evol.*
490 2013;31:474-483.
491 42. Adebesin F, et al. Emission of volatile organic compounds from petunia flowers is facilitated by an
492 ABC transporter. *Science*. 2017; 356:1386-1388.
493 43. Hao R, Yang R, Zhang Z, Zhang Y, Chang J, Qiu C. Identification and specific expression patterns in
494 flower organs of ABCG genes related to floral scent from *Prunus mume*. *Sci. Hortic*.
495 2021;288:110218.
496 44. Yang P, Smalle J, Le7]e S, Yan N, Emborg TJ, Vierstra RD. Ubiquitin C-terminal hydrolases 1 and 2
497 affect shoot architecture in Arabidopsis. *Plant J*. 2007;51:441-457.
498 45. Figueroa CM, Lunn JE. A Tale of Two Sugars: Trehalose 6-Phosphate and Sucrose. *Plant Physiol*.
499 2016;172:7-27.

46. Wang C, Duan W, Ramuli Maquina Riquicho A, Jing Z, Liu T, Hou X, Li Y. Genome-wide survey and expression analysis of the *PUB* family in Chinese cabbage (*Brassica rapa* ssp*. pekinesis*). *Mol. Genet. genom*. 2015;290:2241-2260.
47. Swaminathan K, Peterson K, Jack T. The plant B3 superfamily. *Trends Plant Sci*. 2008;13:647-655.
48. Hayama R, Yang P, Valverde F, Mizoguchi T, Furutani-Hayama I, Vierstra RD, Coupland G. Ubiquitin carboxyl-terminal hydrolases are required for period maintenance of the circadian clock at high temperature in Arabidopsis. *Sci. Rep*. 2021;9:17030.
49. Forrest JRK. Plant – pollinator interactions and phenological change: what can we learn about climate impacts from experiments and observations? *Oikos*. 2005;124:4-13.
50. Hegland SJ, Nielsen A, Lázaro A, Bjerknes AL, Totland Ø. How does climate warming affect plant-pollinator interactions? *Ecol. Lett*. 2009;12:184-195.
51. Fishman L, Kelly AJ, Willis JH. Minor quantitative trait loci underlie floral traits associated with mating system divergence in mimulus. *Evolution*. 2002;56:2138–2155.
52. Fishman L, Beardsley PM, Stathos A, Williams CF, Hill JP. The genetic architecture of traits associated with the evolution of self-pollination in Mimulus. *New Phytol*. 2015;205:907–917.
53. Campitelli BE, Kenney AM, Hopkins R, Soule J, Lovell JT, Juenger TE. Genetic mapping reveals an anthocyanin biosynthesis pathway gene potentially influencing evolutionary divergence between two subspecies of scarlet gilia (*Ipomopsis aggregata*). *Mol. Biol. Evol*. 2017;35:807–822.
54. Bolnick DI, Barrett RDH, Oke KB, Rennison DJ, Stuart YE. (Non)Parallel Evolution. *Ann. Rev. Ecol. Evol. Syst*. 2018;19:303-330.
55. Schmutz J, et al. A reference genome for common bean and genome-wide analysis of dual domestications. *Nat. genet*. 2014;46:707-713.
56. Takuno S, Ralph P, Swarts K, Elshire RJ, Glaubitz JC, Buckler ES, Hufford MB, Ross-Ibarra J. Independent molecular basis of convergent highland adaptation in maize. *Genetics*. 2015;200:1297-1312.
57. Cai L, Comont D, MacGregor D, Lowe C, Beffa R, Neve P, Saski C. The blackgrass genome reveals patterns of non-parallel evolution of polygenic herbicide resistance. *New Phytol*. 2023;237:1891-1907.
58. James ME, Wilkinson MJ, Bernal DM, Liu H, North HL, Engelstädter J, et al. Phenotypic and genotypic parallel evolution in parapatric ecotypes of *Senecio*. *Evolution*. 2021;10:1111-evo.14387.
59. Laurie CC, Chasalow SD, LeDeaux JR, McCarroll R, Bush D, Hauge B, Lai C, Clark D, Rocheford TR, Dudley JW. The genetic architecture of response to long-term artificial selection: for oil concentration in the maize kernel. *Genetics*;168:2141-2155.
60. Pritchard JK, Di Rienzo A. Adaptation – not by sweeps alone. *Nat. Rev. Genet*. 2010;11:665–667.
61. Csilléry K, Rodriguez-Verdugo K, Rellstab C, Guillaume F. Detecting the genomic signal of polygenic adaptation and the role of epistasis in evolution. *Mol. Ecol*. 2018;27:606-612.
62. Barghi N, Hermisson J, Schlötterer C. Polygenic adaptation: a unifying. *Nat. Rev. Genet*. 2020;21:769-781.
63. Barton NH, Etheridge AM, Véber A. The infinitesimal model: Definition, derivation, and implications. *Theor. Popul. Biol*. 2017;118:50-73.
64. Sheng Z, Pettersson ME, Honaker CF, Siegel PB, Carlborg O. Standing genetic variation as a major contributor to adaptation in the Virginia chicken lines selection experiment. *Genome Biol*. 2015;16:219.
65. Berg JJ, Coop G. A population genetic signal of polygenic adaptation. *PloS Genet.* 2014;10:e1004412.
66. Boyle EA, Li YI, Pritchard J K. An expanded view of complex traits: from polygenic to omnigenic. *Cell*. 2017;169:1177-1186.

67. Wieters B, Steige KA, He F, Koch EM, Ramos-Onsins SE, Gu H, et al. Polygenic adaptation of rosette growth in *Arabidopsis thaliana. PloS Genet*. 2021;17:e1008748.
68. El-Esawi MA. Genetic diversity and evolution of Brassica genetic resources: from morphology to novel genomic technologies – a review. *Plant Genet. Resour*. 2017;15:388–399.
69. Danecek P, Auton A, Abecasis G, Albers CA, Banks E, DePristo, et al. The variant call format and VCFtools. J. *Bioinform.* 2011;27:2156–2158.
70. Revell LJ. learnPopGen: An R package for population genetic simulation and numerical analysis. *Ecol. Evol*. 2019;97896–7902.
71. Benjamini Y, Hochberg Y. Controlling the false discovery rate: a practical and powerful approach to multiple testing. *J. R. Stat. Soc. Series B*. 1995;57:289-300.
72. Gabriel SB, et al. The structure of haplotype blocks in the Human genome. *Science*. 2002; 296:2225-2229.
73. Privé F, Luu K, Vilhjálmsson BJ, Blum MGB. Performing highly efficient genome scans for local adaptation with R package pcadapt version 4. *Mol. Biol. Evol*. 2020;37:2153–2154.
74. Wickham H, et al. Welcome to the tidyverse. *J. Open Source Softw*. 2019;4:1686.
75. Rowlingson B, Diggle P. splancs: Spatial and Space-Time Point Pattern Analysis. *R package version 2.01-43*. 2022;https://CRAN.R-project.org/package=splancs

Figure titles and legends

Figure 1. Experimental evolution design. Partial experimental evolution design from Gervasi and Schiestl [12] from the first generation (G1) to the ninth generation in control (C9) and bumblebee treatment (B9). The tenth generation was obtained by inter-replicate crossing (C10 and B10). Population of *Brassica rapa* fast cycling used for seedling sequencing are coloured. The abbreviation and the colours assigned to the populations are unchanged along the manuscript. The number of seedlings (n) sequenced per population is indicated. Images: courtesy of F. Schiestl and L. Frachon.

Figure 2. Allele frequency changes during experimental evolution. (**A**) Comparison of the allele frequency changes (Δh) between the bumblebee treatment (*x-axis*) and the control treatment (*y-axis*). The grey dots represent the 4'713 SNPs. Replicate A is in light grey, replicate B in darker grey. The significant changes are highlighted in blue and green (see the legend in the figure for details). Comparison of initial (first generation) and final (ninth generation) allele frequencies in the control treatment for both replicate A **(B)** and replicate B **(D)**, and in the bumblebee treatment for both replicate A **(C)** and replicate B **(E)**. The grey dots represent the non-significant changes in allele frequencies between generations. The grey solid lines indicate the maximum (upper line) or minimum (lower line) of final simulated allele frequencies obtained by 10'000 simulations of random genetic drift (over nine generations, N_e=16). The color dots represent important changes with *fdr* < 0.05.

588 **Figure 3. Intersection of genomic variants under selection between treatment and replication.** The
589 UpSet plot illustrates the genomic variants involved in the evolution of *Brassica rapa* in control and
590 bumblebee treatment for both replicates A and B. On the left (Set Size), the number of significant
591 genomic variants involved in evolutionary response of *B. rapa* in different populations is indicated. The
592 dots indicate that the genomic variants are involved in the evolutionary response only in a particular
593 population, while the vertical lines indicate that the genomic variants are involved in the evolutionary
594 processes in several populations. The number of genomic variants involved in unique population or in
595 different populations is indicated in the upper part of the figure.
596
597 **Figure 4. Genome-wide population structure. (A) Eigenvalues of the 15 principal components of the**
598 **genomic PCA based on 4713 SNPs. (B-D)** Position of the 256 individuals in the genomic space from the
599 principal component analysis (PCA) performed on their genotypes (GT). The label of the population is
600 shown on their centroid. Polygons linking outer points of the scatter plot are displayed for all
601 populations. The legend colours are indicated in the bottom of the figure.
602
603
604